www.springer.com/41230
https://doi.org/10.1007/s41230-024-4050-5
Research & Development Vol. 22 No. 3 May 2025 CHINA FOUNDRY

Microstructural evolution and mechanical properties of Ti43Al alloy by directional annealing

Li Zhou[1], *Jie-ren Yang[1], Yun-lu Ma[1], Ze-dong Liu[1], and Rui-run Chen[2]

1. College of Materials Science and Engineering, Sichuan University, Chengdu 610065, Sichuan, China

2. School of Materials Science and Engineering, Harbin Institute of Technology, Harbin 150001, Heilongjiang, China

Abstract: The directional annealing technique is widely used to prepare columnar grains or single crystals. To investigate the effect of hot zone temperature and temperature gradient on the growth of columnar crystals, Ti43Al alloys were heat treated by the directional annealing technique and their mechanical properties were tested. The results show that columnar grains with a maximum size of 22.29 mm can be obtained at a hot zone temperature of 1,350 °C and a temperature gradient of 8 K·mm^{-1}. During the directional annealing process, Ti43Al alloys are heated to α single-phase domain to start the phase transformation. Columnar grains with a microstructure of fully lamellar colonies are obtained at different hot zone temperatures and temperature gradients. The distribution of the orientation difference for the α_2 phase was found to be more random, suggesting that the growth of the columnar crystals may be stochastic in nature. Tensile testing results show that the strength and elongation of directional annealed Ti43Al alloy at 1,400 °C-8 K·mm^{-1} are 411.23 MPa and 2.29%, and the remaining directional annealed alloys show almost plasticity.

Keywords: TiAl alloys; directional annealing; microstructural evolution; EBSD, mechanical properties

CLC numbers: TG146.23 **Document code:** A **Article ID:** 1672-6421(2025)03-273-10

1 Introduction

TiAl-based alloys have a broad prospect and become the optimal candidate for superalloys in the fields of aerospace and gas turbines, due to their attractive properties such as low density, high specific strength, and good creep resistance [1-5]. Especially, the directionally solidified TiAl alloys with columnar grains or single crystals, exhibit excellent room-temperature ductility and enhanced high-temperature mechanical properties [6-7].

Up to the present, mainly four pathways can prepare directionally solidified TiAl alloys: (1) traditional Bridgman solidification [8]; (2) optical floating zone melting (OFZM) [9-10]; (3) electromagnetic constraining shaping [11]; (4) cold crucible directional solidification technique (CCDS) [6, 12]. However, the TiAl alloy melt has great chemical activity, which is easy to react with the crucible materials and introduce impurities [8, 13, 14]. In the OFZM and CCDS, melt contamination can be avoided, but the operation process is complex and the directional microstructure is difficult to control [6, 8, 15].

In recent years, some researchers have developed directional annealing to prepare columnar grains in metals [16-18]. The TiAl specimen is fixed on a lifting platform and induction-heated to a higher temperature below the melting point. As the effective heat treatment area moves, non-preferred grains are eliminated and these grains with specific orientations continuously grow. For instance, Ukai et al. [19] prepared zone annealed in a Ni-based oxide dispersion-strengthened (ODS) superalloy, they found that grains with the texture of cube orientation (001)[0$\bar{1}$0] as well as Goss orientation (110)[001] preferentially grew into columnar grains. By controlling the hot zone temperature in β single-phase region and withdrawing rate, columnar grains could be obtained [17]. The plasticity of Ti44Al6Nb1Cr alloy prepared by Liu [20] was improved after directional annealing, which show an improved elongation of 2.3% at room temperature.

In this work, the DA for Ti43Al (at.%) alloys in α

***Jie-ren Yang**

Male, Ph.D., Professor. His research interests mainly focus on high-temperature metal material design, phase transition theory, structure-property control and solidification processing.

E-mail: yangjieren@scu.edu.cn

Received: 2024-03-14; Revised: 2024-06-13; Accepted: 2024-07-02

single-phase region was investigated. To avoid the emergence of β-phase and complex metamorphism in the cooling process and to reduce the resistance to grain boundary migration to promote grain growth, this work set different hot zone temperatures of directional annealing experiments in the α single-phase region. The key influence factors including the temperature of the effective hot zone (1,300, 1,350 and 1,400 °C) and the temperature gradient (approximately 20 and 8 $K\cdot mm^{-1}$) were investigated. The microstructures involving grain morphology, and phase orientation were analyzed. Meanwhile, the formation principle of columnar grains was revealed. Furthermore, the mechanical properties and fracture morphologies of directional annealed Ti43Al were analyzed.

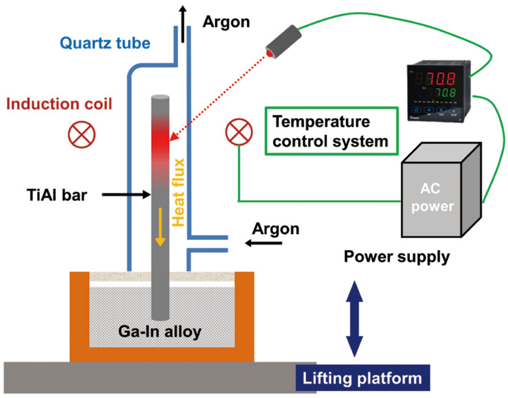

Fig. 1: Schematic diagram of directional annealing of TiAl bars

2 Experiment procedures

2.1 Preparation of Ti43Al master alloy

Ti43Al alloy (at.%) ingot was firstly prepared by vacuum arc remelting twice. Then the ingot with a weight of ~8 kg was remelted by cold crucible induction melting once. The chemical composition of the alloy was determined by inductively coupled plasma atomic emission spectrometry (ICP-AES), as shown in Table 1. The Ti43Al alloy bars, with the size of Φ8 mm×170 mm, for the following directional annealing were wire-cut from the ingot. All the surface of Ti43Al bars was carefully polished with #400 sandpaper to remove the oxidation layer.

Table 1: Element content of Ti43Al alloy in this work (at.%)

Ti	Al	O
57.04	42.86	0.10

2.2 Directional annealing for Ti43Al alloy

Ti43Al alloy bars were fixed on the directional heat treatment equipment, as shown in Fig. 1. The gallium-indium alloy liquid has high thermal conductivity, when the bottom of the bar was submerged in the gallium-indium alloy liquid, the temperature gradient can be adjusted by changing the amount of gallium-indium alloy liquid, and an average temperature gradient of about 20 $K\cdot mm^{-1}$ was formed between the bottom of the bar and the effective heat-treatment zone on the bar; when the bottom of the bar and the gallium-indium alloy liquid did not come into contact with each other, the average temperature gradient was about 8 $K\cdot mm^{-1}$. An infrared thermometer (ISR 6 Advanced, Range: 800–2,500 °C) was used to measure the maximum temperature of the hot zone on the TiAl bars. The temperature control system was self-adjustable, it could ensure a stable preset temperature of the hot zone. The quartz tube was filled with argon to prevent oxidation during directional annealing. The hot zone moved from top to bottom as the platform began to upward lift.

Combined with the titanium-aluminum binary phase diagram [21], the experimental parameters of directional annealing performed in this work are shown in Fig. 2. The annealing temperatures of 1,300, 1,350, and 1,400 °C, were located at the bottom, middle, and top in the α single-phase region, respectively. Before directional annealing, it took 3 min to heat to the preset annealing temperatures, and then 5 min for an isothermal treatment, which can homogenize the single-phase microstructure and reduce the original micro-segregation. The moving rate was set to 4.2 $\mu m\cdot s^{-1}$ and the vertical moving distance for directional annealing was 65–70 mm. Natural cooling under the argon atmosphere was performed after directional annealing, and the cooling rate was estimated to be 600–800 $°C\cdot min^{-1}$.

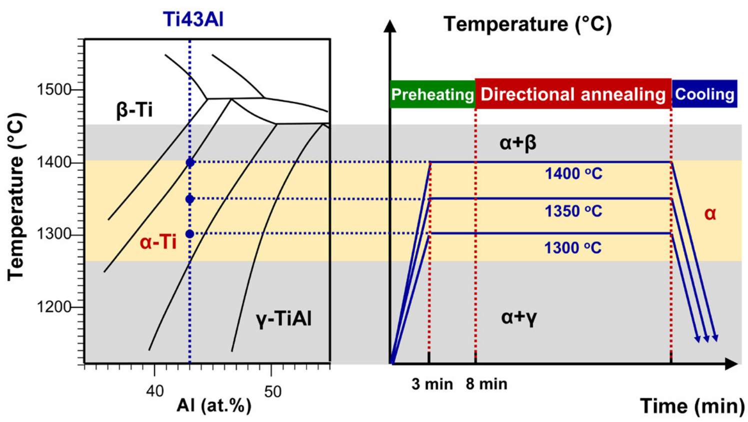

Fig. 2: Part of Ti-Al binary phase diagram [21] and the experimental parameters of directional annealing

2.3 Testing and characterization

After the directional heat treatment, the samples were cut along the longitudinal section, half of which were polished to analyze the annealed microstructures, and the other half was cut for the tensile testing. The feature of grains was observed by an optical microscope (OM) (Axio Observer 3m). The directionally annealed microstructures and their fracture morphologies were characterized by a scanning electron microscope (SEM) (Hitachi SU8010) equipped with a back-scattered electron (BSE) detector. Meanwhile, the electron backscattered diffraction (EBSD) was applied to measure the phase orientation. The lengths and widths of columnar grains were gauged by Image-Pro Plus software. The tensile properties of annealed Ti43Al bars were determined on an electro-mechanical universal testing machine (D series, Sinotest, China). The dimensions of these tensile specimens are shown in Fig. 3. The fracture morphology of tensile specimens was observed by a scanning electron microscope (SEM).

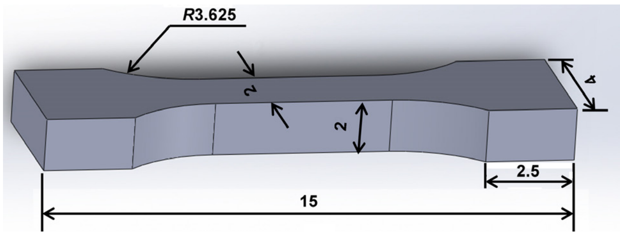

Fig. 3: Dimensions of tensile specimens (unit: mm)

3 Results and discussion

3.1 Directionally annealed microstructures

Macrostructures of as-cast Ti43Al alloy are shown in Fig. 4. The grains are irregular and approximately equiaxed with a rough size of 470.96 μm. A large variation exsits in the shape and size of the grains: some grains are more elongated and others are close to equiaxed. Each grain contains only one directionally aligned lamellar cluster, and some neighboring grains have closer lamellar orientations and smaller misorientations. Many black dots, which distribute nonuniformly, indicate that a large number of holes exist in the as-cast alloy, and these holes can cause the low strength of the tensile specimens after directional annealing [17].

Directionally annealed microstructures are shown in Fig. 5. The equiaxed grains transform into columnar grains. A transition zone exists in the cross-section of the specimen (marked as a blue dashed box in Fig. 5), in which the grains still maintain the equiaxial crystal morphology, but the size is significantly larger than that of the as-cast grains. The length of the transition region tends to decrease with increasing the temperature under the same temperature gradient. It needs to be pointed out that restricted by sampling length, the length of transition region in 1,350 °C-8 $K\cdot mm^{-1}$ seems to be shorter than that in 1,400 °C-8 $K\cdot mm^{-1}$. Furthermore, the transition zone displays a little shorter at larger temperature gradients under the same temperature. The transition region having a minimum length of 6 mm may be explained as follows: the top of the alloy bar is fixed in the middle of the induction coil (width: 15 mm) and moves from this position. Therefore the actual initial effective heating length is about 7.5 mm, which is coincide with the length of the intial transition region. During the preheating, the grains grow freely in all directions. Then the lifting platform moves upward, and the grain boundaries of some specific grains transfer forward along the direction of the hot zone, leading to the columnar grains.

The visible columnar grains are all generated in the specimen cross-section. Except for some columnar grains, most of them extend too wide and terminate at the sample edge, that is why them seems to be short and small. Actually, near the edge of the specimen on both sides, there are no long columnar grains could be observed, almost all short grains. The maximum dimension of columnar grains is 22.29 mm after the directional annealing of 1,350 °C-8 $K\cdot mm^{-1}$, while 18.16 mm after directional annealing of 1,400 °C-8 $K\cdot mm^{-1}$ (These two grains are indicated by red lines in the Fig. 5, and the remaining columnar grains are indicated by yellow lines). The dimensions of the columnar grain are generally consistent with directional annealed $Ti_{44}Al$ prepared by Liu [17] and a single crystal obtained by Chen [9] using an optical floating zone furnace. Apparently, the dimensions of columnar grains, both in length and width, are positively correlated with the temperature at both temperature gradients.

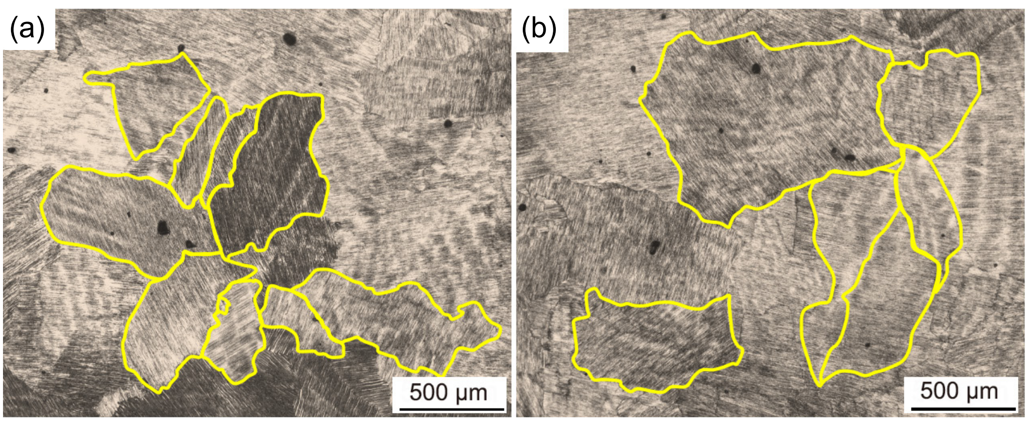

Fig. 4: Macrostructures of as-cast Ti43Al alloy: (a) and (b) denote grains with different morphologies

Some grains in Fig. 5(f) display a more pronounced bulk Widmanstätten laths (i.e. a type of microstructure in which variants of lamellar areas with different orientations are embedded in a lamellar colony matrix) inside the grains. The reason for this microstructure may be that the temperature measuring infrared rays does not accurately hit the maximum temperature region, the actual maximum temperature of the sample exceeds 1,400 °C which is set by the infrared thermometer and the temperature control system, resulting that the microstructures are actually in the (α-Ti+β-Ti) two-phase region, and the β-α phase transition occurs in the very slow cooling process (the cooling rate is less than 50 $°C·min^{-1}$) [22]. In addition, the largest size of columnar grains appear after the directional annealing of 1,350 °C-8 $K·mm^{-1}$, which can be seen in Fig. 5(e), where the lamellar orientation inside the columnar grains is almost perpendicular to the growth direction, and the lamellar orientation of the rest of the columnar grains in this sample also has a relatively larger angle compared with other specimens. It indicates that the growth of columnar grains in the directional annealing technique has little relationship with the lamellar orientation, and the lamellar orientation is not an important factor in determining whether the grain boundary can be pushed forward.

The microstructures of directional annealed Ti43Al alloys are shown in Fig. 6. The average lamella spacing of the alloys after directional annealing at 1,300, 1,350, and 1,400 °C under a temperature gradient of 8 $K·mm^{-1}$ is 834, 914, and 666 nm, as shown in Figs. 6(a–c), respectively; the average lamella spacing the alloys after directional annealing at 1,300, 1,350, and 1,400 °C under a temperature gradient of 20 $K·mm^{-1}$ is 806, 736, and 630 nm [Figs. 6(d–f)], respectively. Under the same temperature gradient, different heating temperatures have an effect on the lamella spacing, and it shows that the lamella spacing is minimized at the highest temperature. It is obvious that the lamella spacing of the alloys after directional annealing under a temperature gradient of 8 $K·mm^{-1}$ slightly increases comparing with those under a temperature gradient of 20 $K·mm^{-1}$ at the same hot zone temperature. In γ-TiAl alloys, the lamellar spacing is mainly determined by the lamellar spacing of the γ phase, which is mainly related to the cooling rate and the withdrawing rate. During directional annealing, the cooling rate is equal to the product of the temperature gradient and the withdrawing rate. In the case of the same annealing temperature, constant argon flow rate, and the same temperature gradient of directional annealing, the greater the withdrawing rate is, the larger the cooling rate is. An increase in the cooling rate results in a lower onset temperature for the γ phase to begin to precipitate and an increase in supercooling degree, which ultimately leads to an increase in the nucleation rate of the γ phase. In addition, the increasing cooling rate can lead to the shorter residence time of the grains in the high-temperature region, so the diffusion rate

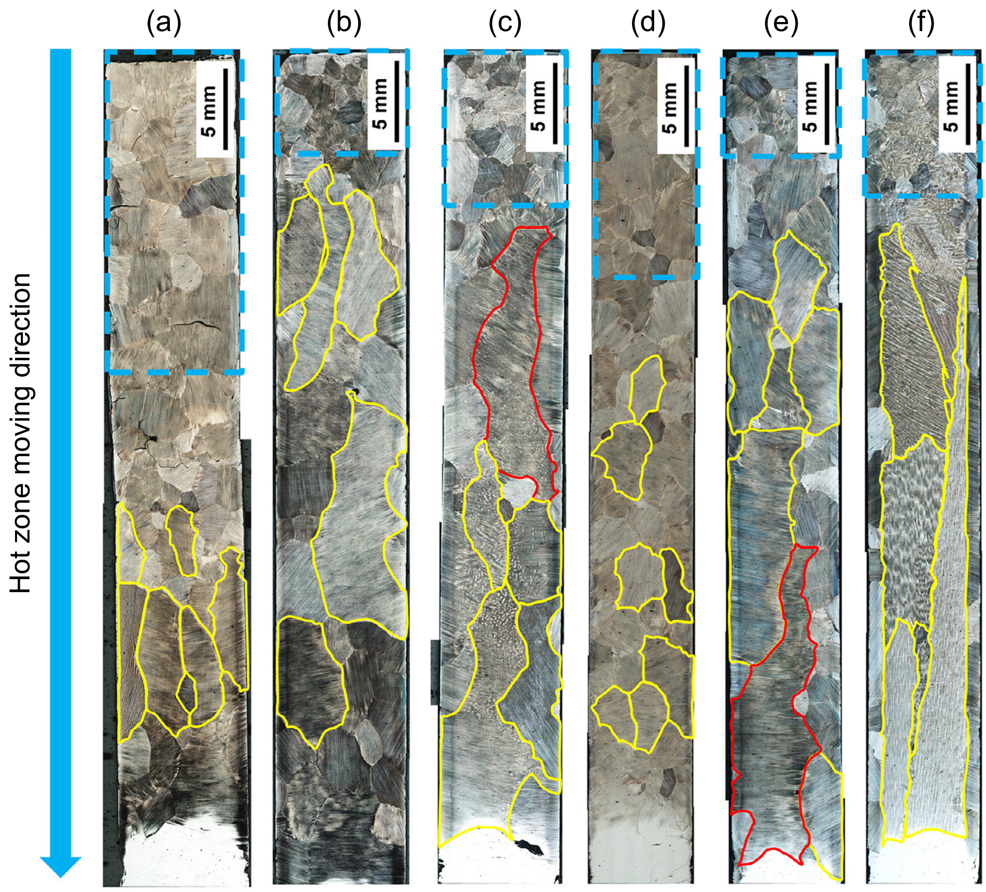

Fig. 5: Macrostructures of DA-Ti43Al alloys under different parameters of directional annealing: (a) 1,300 ºC-20 $K·mm^{-1}$; (b) 1,350 ºC-20 $K·mm^{-1}$; (c) 1,400 ºC-20 $K·mm^{-1}$; (d) 1,300 ºC-8 $K·mm^{-1}$; (e) 1,350 ºC-8 $K·mm^{-1}$; (f) 1,400 ºC-8 $K·mm^{-1}$ (Both red and yellow lines indicate columnar grains, where the red lines indicate the two grains of larger size, and blue dashed boxs indicate growth transition zones)

of the atom becomes lower, and γ lamellar layer is too late to thicken to a certain extent. Therefore, the faster the cooling rate, the finer the lamellar microstructure forms.

The lamellar orientation of all grains is labeled in Fig. 7. The lines with different colors stand for the direction difference between the lamellar phase orientation and the growth direction of columnar grains. The green lines indicate 0°–30°, yellow lines indicate 30°–60°, and red lines indicate 60°–90°. Grains of all lamellar orientations have the potential to grow into columnar grains along the direction of heat flow. However, the distribution of the three colors is not completely random, and some concentrated areas indicate that there are similarly oriented grains near these larger-sized columnar grains. This indicates that the grains with similar lamellar orientation are more likely to grow synergistically. For the columnar grains that are labeled in Fig. 7, the lamellar orientation of most grains is labeled as red or yellow, and only a few columnar grains are labeled as green, indicating that the grains with a larger angle between the lamellar orientation and the growth direction have the possibility of preferential growth. Some

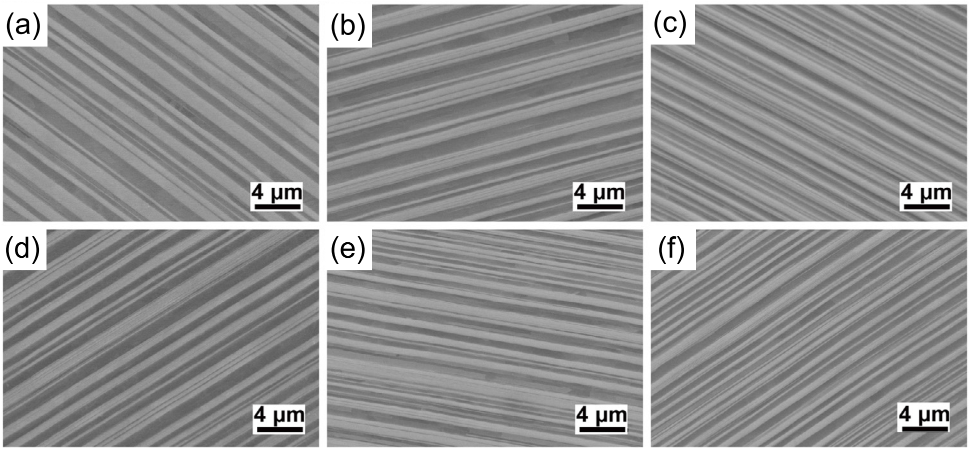

Fig. 6: BSE of DA-Ti43Al alloys under different parameters of directional annealing: (a) 1,300 °C-8 K·mm^{-1}; (b) 1,350 °C-8 K·mm^{-1}; (c) 1,400 °C-8 K·mm^{-1}; (d) 1,300 °C-20 K·mm^{-1}; (e) 1,350 °C-20 K·mm^{-1}; (f) 1,400 °C-20 K·mm^{-1}

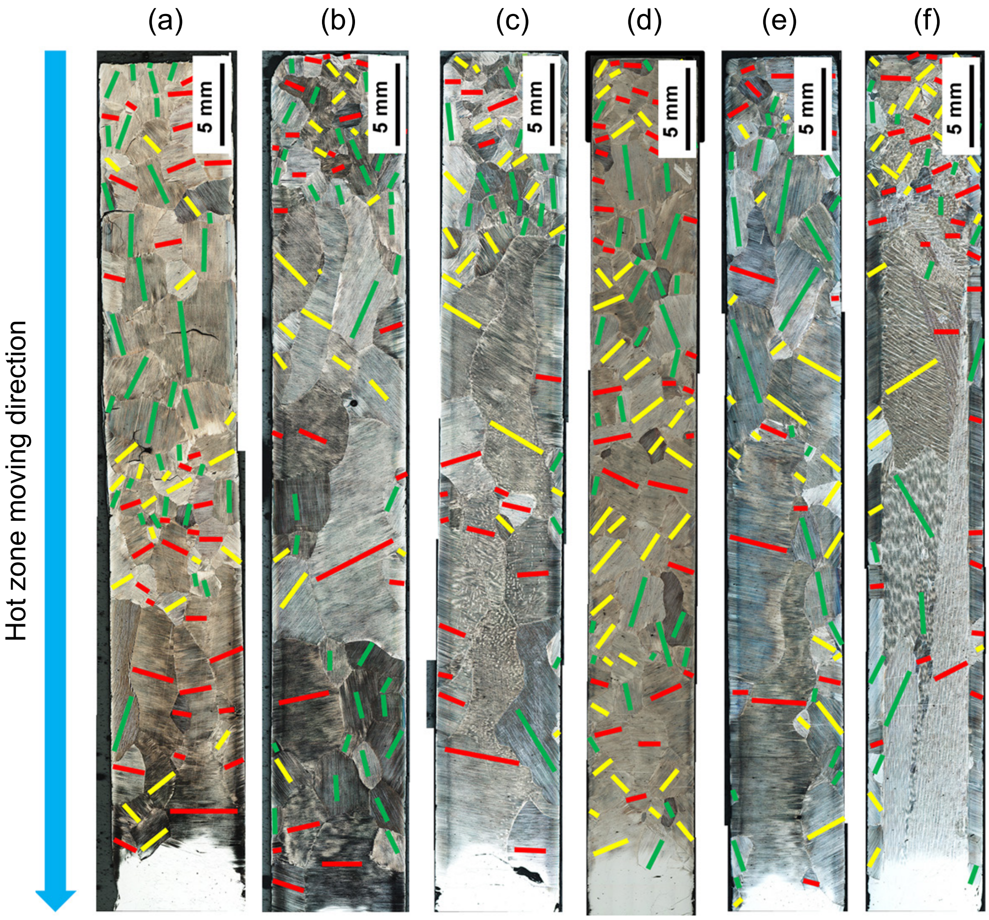

Fig. 7: Lamellar orientation of DA-Ti43Al alloys under different parameters of directional annealing: (a) 1,300 ºC-20 K·mm^{-1}; (b) 1,350 ºC-20 K·mm^{-1}; (c) 1,400 ºC-20 K·mm^{-1}; (d) 1,300 ºC-8 K·mm^{-1}; (e) 1,350 ºC-8 K·mm^{-1}; (f) 1,400 ºC-8 K·mm^{-1} (Green line means the direction difference within 0°–30°, red line means within 30°–60°, and yellow line means within 60°–90°)

columnar grains and the equiaxed grains at their fronts are selected to calculate the lamellar misorientation, and the results show that the lamellar misorientation is large, all of which are larger than 48°. It can be tentatively concluded that two neighboring grains with large lamellar misorientation may hinder the migration of grain boundaries along the moving direction of the hot zone.

3.2 Orientation analysis

The microstructures of the as-cast TiAl alloy are approximately equiaxed grains, and after directional annealing, some of the grains grow along the direction of the hot zone to form columnar elongated grains. In order to figure out the mechanism of these grain growth, the columnar grains (which are marked with yellow lines in Fig. 8) and the small grains at their growth fronts (whose sizes are smaller than those of the columnar grains, are marked with green lines in Fig. 8) are selected for EBSD. The maximum temperatures in the effective heat treatment zones in this experiment are all within the α single-phase zone. Theoretically, following the phase transition path of the phase diagram, in the whole process of effective heat treatment, a grain undergoes $(\alpha_2+\gamma)_1$, α, (α+γ), $(\alpha_2+\gamma)_2$ phase domains in turns, where $(\alpha_2+\gamma)_1$ refers to the as-cast structure, $(\alpha_2+\gamma)_2$ refers to the structure after directional annealing. The formation of γ lamellae starts after entering the (α+γ) two-phase region during the cooling process. As the temperature continues to decrease to the eutectic temperature, the α to α_2 ordering transition occurs while the γ lamellae continue to precipitate, forming the $(\alpha_2+\gamma)_2$ phase. Nevertheless, due to the small aluminum content of the Ti43Al alloy (less than 44at.%) [23, 24], the actual phase transition is $(\alpha_2+\gamma)_1$, α, α_2, $(\alpha_2+\gamma)_2$. The orientation of the α_2 phase formed during the cooling is consistent with the high-temperature α phase, so misorientation of the α_2 phases is only considered within each grain.

Typical columnar grains and the equiaxed grains at the growth front are selected for EBSD analysis, expecting to derive the misorientation between the α_2 phase of these two grains, and to further summarize the laws of grain growth in terms of orientation. As depicted in Fig. 8(a), the experimental parameters are 1,300 °C-8 K·mm^{-1} on the sample, the columnar grains are grains 1, 2, and 3, and the equiaxed grains in front of them are 4, 5, 6, and 7, and their respective corresponding crystal information is derived [labeled in Fig. 8(b)], and finally the misorientation between each columnar grain and

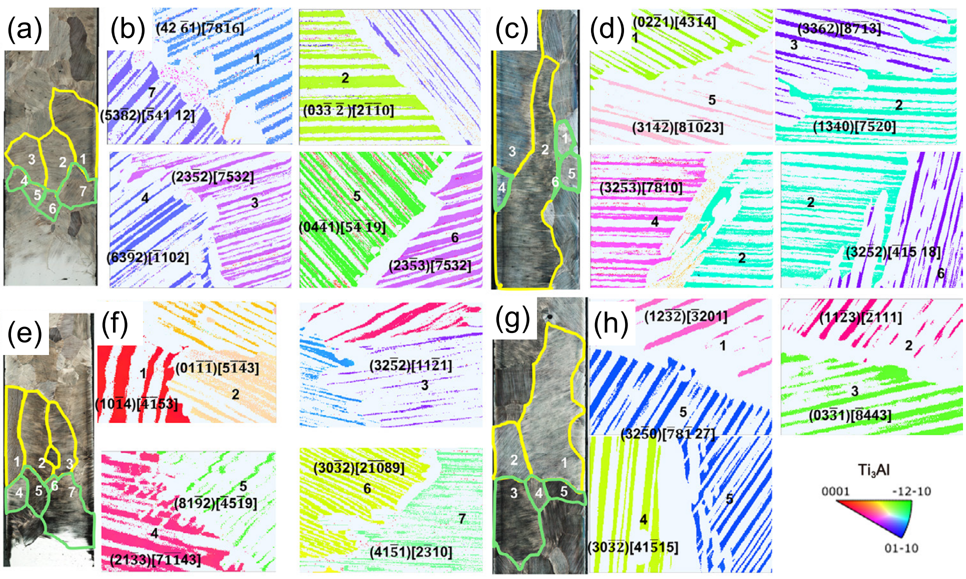

Fig. 8: EBSD of columnar grains and the equiaxed grains at the growth front: (a, b) 1,300 °C-8 K·mm^{-1}; (c, d) 1,350 °C-8 K·mm^{-1}; (e, f) 1,300 °C-20 K·mm^{-1}; (g, h) 1,350 °C-8 K·mm^{-1}

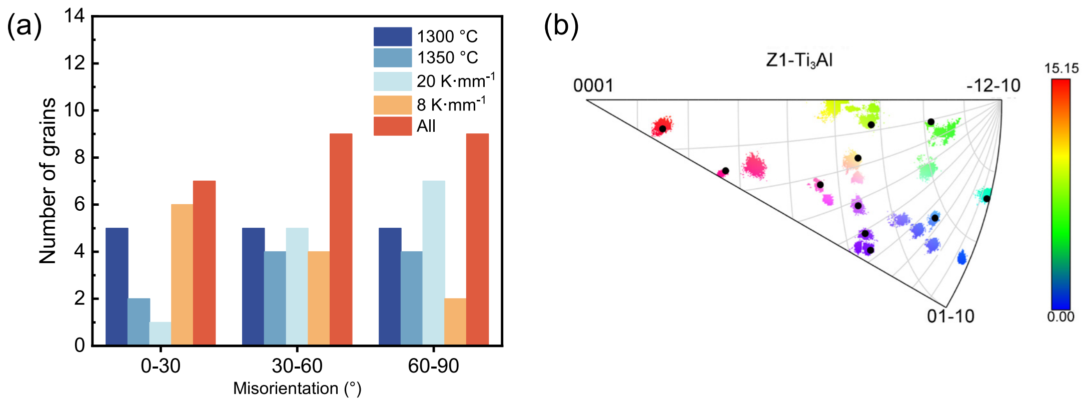

Fig. 9: EBSD results for directional annealed Ti43Al alloys: (a) statistics results of orientation difference; (b) inverse pole figure (IPF)

the neighboring equiaxed grains is calculated. Finally, all the misorientations are categorized by angular size and plotted as a histogram (Fig. 9).

All of the misorientation results were organized separately by hot zone temperature and temperature gradient and plotted as a bar graph [shown in Fig. 9(a)]. Looking at the first two columns of the bar graph, that is, when the hot zone temperature is used as a variable, the change in the magnitude of the misorientation angle between the three angular intervals is not significant, indicating that changing temperature does not affect the misorientations between the grains. However, under the same hot zone temperature, when the temperature gradient is 20 $K\cdot mm^{-1}$, the orientation difference between columnar grains and neighboring grains is mostly larger than 30°, and when the temperature gradient is smaller (8 $K\cdot mm^{-1}$), half of the orientation difference is smaller than 30°, showing opposite distribution trends. Finally, by combining all the orientation differences, 40% phase orientation keeps in 0°–30° orientation difference, 36% phase orientation keeps in 30°–60° and 24% phase orientation keeps in 60°–90°. The actual number of samples selected is small, so there is no obvious pattern in the phase orientation difference.

All grains were plotted synthetically in the inverse pole figure (IPF) [shown in Fig. 9(b)]. Although the number of grain samples tested by EBSD is limited, the results show some regularity. Firstly, the grains are not completely randomly distributed, and the relative overlap of the positions of certain grains in the inverse pole figure suggests that a certain degree of selective orientation does exist in the grain growth process of directional annealing. Although these grains do not preferentially grow into columnar grains, they are probably not engulfed during the growth process and thus can be retained at the columnar grain front. Secondly, the grains in which the black dots are labeled indicate columnar grains, which are more dispersed in the IPF, and some of them are located closer to the remaining equiaxed grains. This indicates that there is randomness in the growth of columnar grains. It also shows that the grains at the front of the columnar grains also have the possibility to grow into columnar grains, only that the growth potential of these grains is not as good as that of the grains that have already become columnar grains.

Figure 10 reveals the schematic diagram of the microstructure evolution of TiAl alloy during directional annealing. The initial microstructure of the specimen is fully lamellar. During preheating, the α single-phase region is found at the hot zone as well as at the hot zone front, original grains in it grow up along all directions to generate bigger equiaxed grains. When directional annealing begins, the induction coil moves down slowly, some specific grain boundaries at the front of the hot zone migrate toward the center of the hot zone, and if this migration rate is consistent with the rate of the hot zone, the grain boundaries keep migrating forward at a steady rate, and ultimately retains the columnar grain form. The growth of columnar crystals is the process by which the α grains at the hot zone grow by engulfing the smaller α grains forward. Meanwhile, there is also a lateral competition between the columnar crystals. With the movement of the hot zone, the

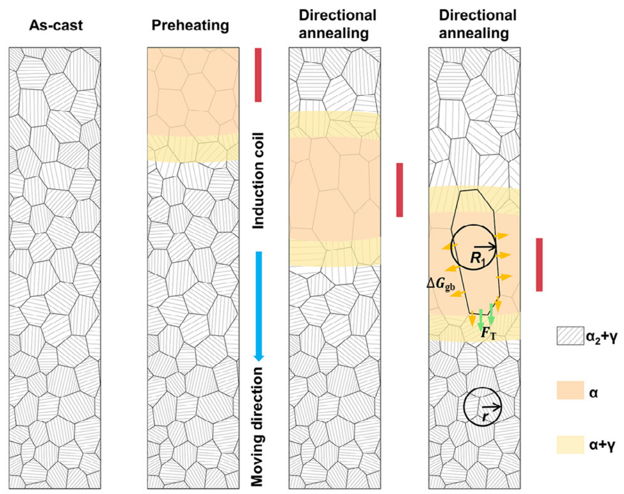

Fig. 10: Schematic diagram of columnar grains growth

newly formed columnar grains gradually leave the hot zone, and the temperature drops slowly to the (α+γ) phase after the γ lamellae begin to nucleate in the original α-phase of the (0001) crystal surface and grow, to be even lower temperature, γ lamellae occurring coarsening. Continue cooling, under a certain supercooling degree, the $\alpha\rightarrow\alpha_2$ disordered-ordered transformation occurs, and ultimately forming the columnar grains with fully lamellar.

The grain-boundary migration velocity, v, according to the Nernst-Einstein relation [25], during directional annealing is given by Eq. (1):

$$v=M\times F \tag{1}$$

where F is the driving force, M stands for the grain boundary mobility, which is given by Eq. (2):

$$M=\frac{b^4\gamma}{kT}e^{\frac{-Q}{RT}} \tag{2}$$

where b=2λ, is approximately equal to the atomic diameter, for titanium atoms, it takes the value of 289.6 pm, 2λ is the grain boundary thickness, and γ represents the atomic jump frequency across the boundary and takes the value of 10^{13} s^{-1} [19]. R stands for the universal gas constant, and Q denotes the activation energy for the atomic diffusion across the boundary. From these two equations, it can be seen that increasing the temperature can lead to an increase in the grain boundary mobility, which in turn leads to an increase in the grain boundary velocity.

The driving force (F) responsible for columnar grain growth comprises two components: the thermal gradient driving force (F_T) and the grain boundary energy difference (ΔG_{gb}). This relationship is defined by Eq. (3):

$$F=F_T+\Delta G_{gb} \tag{3}$$

There are different views on the effect of temperature gradients on directional annealed grain boundary migration. Gottstein and Shvindlerman [26] have suggested that temperature gradients can provide a driving force for the grain boundary migration. While Bai et al. [25] suggest that the rate of grain boundary directional migration is not well correlated with the temperature gradient based on molecular dynamics calculations. But according to the experimental results, the temperature gradient does affect the size of the columnar grains, so the effect of the temperature gradient on the migration dynamics of grain boundaries should be taken into account. Thermal gradient driving force is demonstrated by Eq. (4):

$$F_{\mathrm{T}} = \frac{\Delta S \times 2\lambda}{\Omega_{\mathrm{a}}} \times \frac{\mathrm{d}T}{\mathrm{d}Z} \tag{4}$$

where ΔS is the entropy difference between a grain boundary and a single grain, 2λ is the same sense as the former one in Eq. (2), Ω_{a} is the material molar volume, $\frac{\mathrm{d}T}{\mathrm{d}Z}$ is the thermal gradient. Clearly, the thermal gradient driving force increases with increasing the temperature gradient.

During the directional annealing process, the dimension of the grains in the moving effective heat treatment zone after a certain period of insulation, would be larger than the rest of the original grains without growing. The grain boundary energy difference will provide the energy for the grains to further grow, this energy is expressed as, ΔG_{gb}, which is exhibited by Eq. (5) [27]:

$$\Delta G_{\mathrm{gb}} = 2\gamma\left(\frac{1}{r} - \frac{1}{R_1}\right) \tag{5}$$

where γ is the grain boundary energy of two adjacent grains with equivalent radius r and R_1, respectively, and it generally takes the value of 0.5 J·m^{-2} of a random grain boundary [28]. The initial grain size of as-cast grains, denoted as 'r' is 235.48 μm, and, the equivalent radius of columnar grains after directional annealing, denoted as 'R_1', which is 2.74 mm at 1,400 °C-20 K·mm^{-1} and 3.28 μm at 1,350 °C-8 K·mm^{-1}. Both are indicated in Fig. 10. As listed in Table 2, these values lead to 3.89 MJ·m^{-3} for ΔG_{gb} at 1,400 °C-20 K·mm^{-1} and 3.94 MJ·m^{-3} at 1,350 °C-8 K·mm^{-1}. The grain-boundary migration velocity, v, is finally derived to be 6.25 μ·ms^{-1} at 1,400 °C-20 K·mm^{-1} and 3.89 μ·ms^{-1} at 1,350 °C-8 K·mm^{-1}, which is relatively more comparable to the coil moving velocity. Theoretically, the size of columnar crystals can be maximized when the front end of the columnar grains moves in synchronization with the moving hot zone simultaneously. So the combined consideration of grain-boundary migration velocity and hot zone moving velocity can better explain the fact that columnar crystals with larger longitudinal grain sizes grow at lower temperatures and smaller temperature gradients (1,350 °C-8 K·mm^{-1}).

3.3 Mechanical properties

Tensile test results with different experimental parameters are shown in Fig. 11(a). It indicates that the sample with the annealing temperatures of 1,400 °C and small temperature gradient (8 K·mm^{-1}) has the maximum tensile strength of 411.23 MPa and the elongation of 2.29%, which is much higher than the result of directional annealed Ti44Al alloy with 217 MPa and 1.78% [17]. The tensile strength of the other groups is below 200 MPa, but shows a gradual increase with increasing the annealing temperature under the same temperature gradient, with hardly any plasticity and a complete brittle fracture. A comparison of tensile strength and elongation of some TiAl alloys is presented in Fig. 11(b). By adding alloying elements or Y_2O_3, the four alloys within the green oval have high tensile strength with varying elongation. The directional annealed Ti43Al alloy of 1,400 °C-8 K·mm^{-1} shows a better combination of tensile strength and elongation than the other binary TiAl alloys.

The microstructure of Ti43Al alloys is mainly composed of $\alpha_2(Ti_3Al)$ and γ(TiAl) phases at room temperature and 800 °C. On the one hand, the structure type of $\alpha_2(Ti_3Al)$ is $D0_{19}$ is an ordered HCP structure. There are only three main types of slip systems in the α_2 phase [29-31], namely, the prismatic slip system $<11\bar{2}0>\{10\bar{1}0\}$, the bottom slip system $<11\bar{2}0>\{0001\}$, and the conical slip system $<11\bar{2}6>\{11\bar{2}1\}$, among which the conical slip is the most difficult to slip with the highest critical shear stress. On the other hand, the

Table 2: Calculation results for different directional annealing processes

Annealing process	R (μm)	R_1 (mm)	F_{T} (MJ·m^{-3})	ΔG_{gb} (MJ·m^{-3})	M (m^4·s^{-1}·J^{-1})	v (μm·s^{-1})
1,400 ºC-20 K·mm^{-1}	235.48	2.74	1.74	3.89	1.11×10^{-9}	6.25
1,350 ºC-8 K·mm^{-1}	235.48	3.28	0.695	3.94	8.39×10^{-10}	3.89

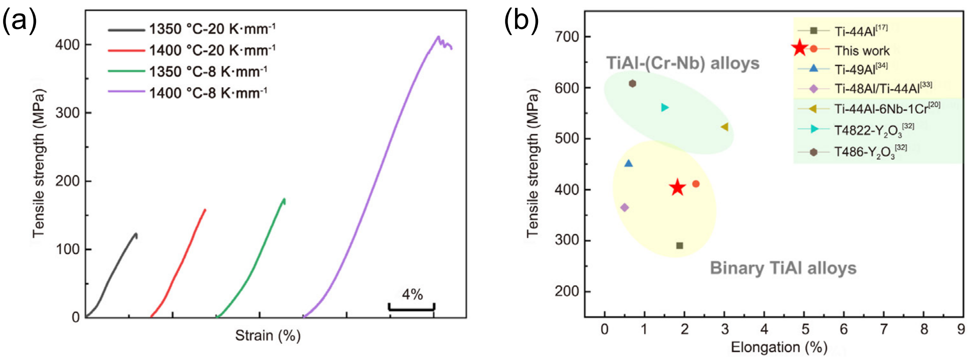

Fig. 11: Mechanical properties of directional annealed Ti43Al alloys: (a) stress-strain curve for tensile testing at 800 °C; (b) a comparison of tensile strength and elongation for TiAl alloys [9, 17, 20, 32, 33]

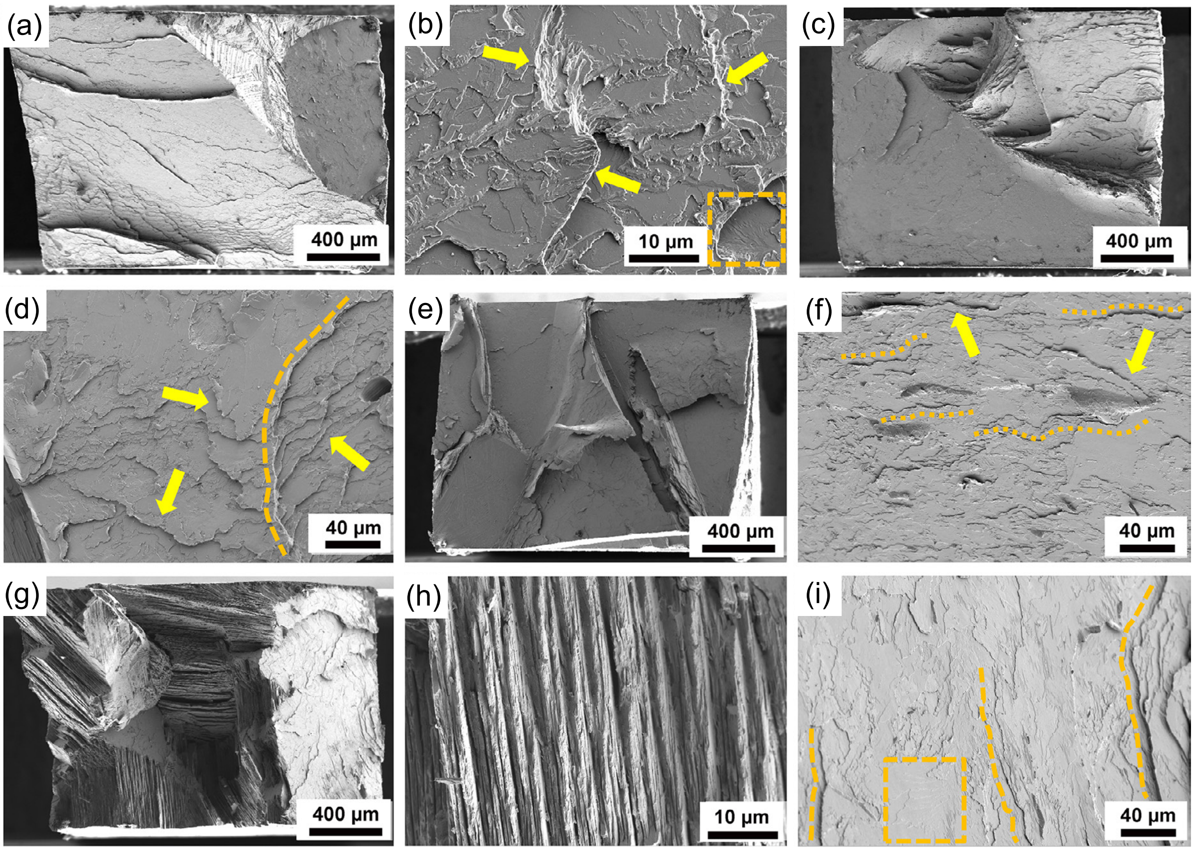

Fig. 12: Fracture morphology of directional annealed Ti43Al alloy under different parameters of directional annealing: (a, b) 1,350 °C-20 K·mm^{-1}; (c, d) 1,400 °C-20 K·mm^{-1}; (e, f) 1,350 °C-8 K·mm^{-1}; (g, h, i) 1,400 °C-8 K·mm^{-1}

structure type of γ(TiAl) is $L1_0$, which is FCC structure. With the large difference between titanium and aluminum atoms in radius, the crystal symmetry of γ-phase is reduced. Hence, Ti43Al alloys have poor plasticity at room temperature.

To further figure out the reason for the mechanical property, the fracture morphology of the specimens was observed (Fig. 12). The specimens after the directional annealing of 1,350 °C-20 K·mm^{-1}, 1,400 °C-20 K·mm^{-1}, and 1,350 °C-8 K·mm^{-1}, as shown in Figs. 12(a, c, and e), are obviously brittle fractures along the lamellae, while the fracture is essentially perpendicular to the lamellae in the specimen after directional annealing of 1,400 °C–8 K·mm^{-1} [Fig. 12(g)]. Figures 12(b, d, and f) further present the details of the brittle fracture mode, where the smoother cleavage surface and locally plasticized tearing edges can be observed, as marked by arrows. This indicates partial plastic fracture behavior, but given the observed ubiquitous flat cleavage surface, these specimen still primarily undergo brittle fracture process. The river patterns, cleavage steps, and tearing ridges can be observed in the fracture morphology. A typical fan-shaped river pattern is shown which is marked in the orange dashed box [Fig. 11(b)]. The crack is centered at a point in the lower right corner and expands in a fan-like shape toward the upper left corner of the dashed box, eventually forming a fan-shaped river pattern. A hole with a size of about 20 μm appears in Fig. 12(d). The tearing edges (outlined with orange dashed on the left side) are more evenly distributed in a transverse direction, whereas the tearing edges on the right side gradually converge in the shape of a river tributary from the upper right to the lower left, and there is a distinct step. The presence of micropores alters the crack extension path and it is possible that some cracks arise from the micropores, resulting in a step pattern with denser tear edges on the right side. The river patterns in Fig. 12(f) clearly extend in a left-to-right direction, suggesting that the cracks arise from the left side expanding to the right. A dissociation pattern similar to a tongue pattern also appears in the figure. Twin crystals may have been present here, and the crack propagates here and deviates from its original extension path along the separation of the matrix and the twin crystals, eventually forming a tongue pattern. A fan-shaped river pattern (in the orange dashed box) also appears in Fig. 12(i). The tearing edges outlined with orange dashed show a longitudinal distribution.

The main reason for these brittle fracture characteristics is that the orientation of the lamellae is close to vertical or at a large angle to the tensile direction. The lamellae orientation of Fig. 12(h) is nearly parallel to the tensile direction, so the fracture morphology is mainly a tearing edge. As is generally known, TiAl polysynthetic twinned (PST) [9] single crystals with the 0° lamellar orientation have a superior tensile ductility of 6.3%–7.6% and a high strength of 930–1,035 MPa at ambient temperature. The fracture morphology and mechanical properties are in good agreement.

4 Conclusions

Ti43Al alloys were prepared under differnet hot zone temperatures and temperature gradients in the directional annealing technique, and their microstructure evolution and mechanical properties were analyzed. This work provides a new idea for improving the microstructures of binary TiAl alloys, which helps to understand and master the microstructure regulation of TiAl alloys in the directional annealing process, and it is of great practical significance for further improving the properties of TiAl alloys. The results can be summarized as follows:

(1) Directional annealing at 1,350 °C and 8 K·mm^{-1} allows the growth of 22 mm columnar grains. The reason is that the difference between the grain boundary migration speed and the hot zone moving speed is minimal, so the grain boundary can be pushed stably.

(2) A large difference in lamellar orientation between two neighboring grains may hinder the migration of grain boundaries in the direction of hot zone movement, and there may be randomness in the growth of columnar grains.

(3) Tensile specimens with lamellae oriented at a small angle to the tensile direction are prepared after directional annealing at 1,400 °C and 8 K·mm^{-1}, reaching a maximum breaking strength of 411.23 MPa and an elongation of 2.29%.

Acknowledgment

This work was supported by the National Natural Science Foundation of China (Grant Nos. 52074229, 52371035), the Key R&D Plan of Sichuan Province (Grant No. SC2022A1C01J), and the State Key Lab of Advanced Metals and Materials (Grant No. 2020-ZD05).

Conflict of interest

Prof. Rui-run Chen is an EBM of *CHINA FOUNDRY*. He was not involved in the peer-review or handling of the manuscript. The authors have no other competing interests to disclose.

References

[1] Clemens H, Mayer S. Design, processing, microstructure, properties, and applications of advanced intermetallic TiAl alloys. Advanced Engineering Materials, 2012, 15(4): 191–215.

[2] Clemens H, Smarsly W. Light-weight intermetallic titanium aluminides–Status of research and development. Advanced Materials Research, 2011, 278: 551–556.

[3] Kim S W, Hong J K, Na Y S, et al. Development of TiAl alloys with excellent mechanical properties and oxidation resistance. Materials & Design, 2014, 54: 814–819.

[4] Kothari K, Radhakrishnan R, Wereley N M. Advances in gamma titanium aluminides and their manufacturing techniques. Progress in Aerospace Sciences, 2012, 55: 1–16.

[5] Liu Y, Hu R, Yang J, et al. Tensile properties and fracture behavior of in-situ synthesized Ti_2 AlN/Ti48Al2Cr2Nb composites at room and elevated temperatures. Materials Science and Engineering: A, 2017, 679: 7–13.

[6] Chen R, Dong S, Guo J, et al. Microstructure evolution and mechanical properties of directionally-solidified TiAlNb alloy in different temperature gradients. Journal of Alloys and Compounds, 2015, 648: 667–675.

[7] Ding H, Wang Y, Chen R, et al. Effect of growth rate on microstructure and tensile properties of Ti-45Al-2Cr-2Nb prepared by electromagnetic cold crucible directional solidification. Materials & Design, 2015, 86: 670–678.

[8] Lapin J, Gabalcová Z, Pelachová T. Effect of Y_2O_3 crucible on contamination of directionally solidified intermetallic Ti-46Al-8Nb alloy. Intermetallics, 2011, 19(3): 396–403.

[9] Chen G, Peng Y, Zheng G, et al. Polysynthetic twinned TiAl single crystals for high-temperature applications. Nature Materials, 2016, 15(8): 876–881.

[10] Lee H N, Johnson D R, Inui H, et al. Microstructural control through seeding and directional solidification of TiAl alloys containing Mo and C. Acta Materialia, 2000, 48(12): 3221–3233.

[11] Johnson D R, Inui H, Yamaguchi M. Alignment of the TiAl/Ti_3Al lamellar microstructure in TiAl alloys by directional solidification. Materials Science and Engineering: A, 1997, 240: 577–583.

[12] Yang J, Chen R, Su Y, et al. Optimization of electromagnetic energy in cold crucible used for directional solidification of TiAl alloy. Energy, 2018, 161: 143–155.

[13] Cui R J, Zhang H R, Tang X X, et al. Interactions between γ-TiAl melt and Y_2O_3 ceramic material during directional solidification process. Transactions of Nonferrous Metals Society of China, 2011, 21(11): 2415–2420.

[14] Liu A H, Li B S, Nan H, et al. Study of interfacial reaction between TiAl alloys and four ceramic molds. Rare Metal Materials and Engineering, 2008, 37(6): 956–959.

[15] Yamaguchi M, Johnson D R, Lee H N, et al. Directional solidication of TiAl-base alloys. Intermetallics, 2000, 8(5): 511–517.

[16] Liu Y, Xue X, Chen R, et al. A novel method to prepare columnar grains of TiAl alloys by controlling induction heating. International Communications in Heat and Mass Transfer, 2019, 108: 104315.

[17] Liu Y, Xue X, Fang H, et al. Microstructure evolution of Ti44Al alloy during directional induction heat treatment and its effect on mechanical properties. Materials Science and Engineering: A, 2020, 772: 138701.

[18] Yang C, Baker I. Directional recrystallisation processing: A review. International Materials Reviews, 2020, 66(4): 256–286.

[19] Ukai S, Taya K, Nakamura K, et al. Directional recrystallization by zone annealing in a Ni-based ODS superalloy. Journal of Alloys and Compounds, 2018, 744: 204–210.

[20] Liu Y, Xue X, Tan Y, et al. Microstructure formation and elevated temperature mechanical properties of directionally solidified Ti44Al6Nb1Cr alloy. Materials Science and Engineering: A, 2020, 797: 140038.

[21] Wu X. Review of alloy and process development of TiAl alloys. Intermetallics, 2006, 14(10–11): 1114–1122.

[22] Hecht U, Witusiewicz V, Drevermann A, et al. Grain refinement by low boron additions in niobium-rich TiAl-based alloys. Intermetallics, 2008, 16(8): 969–978.

[23] Ramanujan R V. Phase transformations in γ based titanium aluminides. International Materials Reviews, 2013, 45(6): 217–240.

[24] Yamabe Y, Takeyama M, Kikuchi M. Determination of α(A3)→α_2(D019) transition temperatures in Ti-(40–45)at%Al alloys. Scripta Metallurgica et Materialia, 1994, 30(5): 553–557.

[25] Bai X M, Zhang Y, Tonks M R. Testing thermal gradient driving force for grain boundary migration using molecular dynamics simulations. Acta Materialia, 2015, 85: 95–106.

[26] Gottstein G, Shvindlerman L S. Grain boundary migration in metals: Thermodynamics, kinetics, applications. Boca Raton: CRC Press, 1999.

[27] Baker I, Li J. Directional annealing of cold-rolled copper single crystals. Acta Materialia, 2022, 50(4): 805–813.

[28] Li J, Baker I. An EBSP study of directionally recrystallized cold-rolled nickel. Materials Science and Engineering: A, 2005, 392(1–2): 8–22.

[29] Inui H, Toda Y, Shirai Y, et al. Low-temperature deformation of single crystal of a D019 compound with an off-stoichiometric composition (Ti-36.5 at.% Al). Philosophical Magazine: A, 1994, 69(6): 1161–1177.

[30] Legros M, Couret A, Caillard D. Prismatic and basal slip in Ti_3Al. I: Frictional forces on dislocations. Philosophical Magazine: A, 1996, 73(1): 61–80.

[31] Legros M, Couret A, Caillard D, Prismatic and basal slip in Ti_3Al. II: Dislocation interactions and cross-slip processes. Philosophical Magazine: A, 1996, 73(1): 81–99.

[32] Guo Y, Chen Y, Xiao S, et al. Influence of nano-Y_2O_3 addition on microstructure and tensile properties of high-Al TiAl alloys. Materials Science and Engineering: A, 2020, 794: 139803 .

[33] Wang Q, Chen R, Yang Y, et al. High-throughput analysis of Al and Nb effects on mechanical behaviour of TiAl alloys using electromagnetic cold crucible continuous casting. Journal of Alloys and Compounds, 2019, 775: 124–131.

[34] Fan J, Wei Z, Li Y, et al. Lamellae orientation control and mechanical properties of directionally solidified binary Ti-49Al alloy in oxide ceramics crucible. International Journal of Metalcasting, 2022, 16(2): 622–633.